01 Jun 1999

Grain Oriented Crystallization, Piezoelectric, and Pyroelectric Properties of (BaxSr2 - X)TiSi2O8 Glass Ceramics

Jianping Zhang

Burtrand I. Lee

Robert W. Schwartz
Missouri University of Science and Technology

Zhenya Ding

Grain oriented crystallization, piezoelectric, and pyroelectric properties of $(Ba_xSr_{2-x})TiSi_2O_8$ glass ceramics

Jianping Zhang, Burtrand I. Lee, and Robert W. Schwartz
Department of Ceramic and Materials Engineering, Clemson University, Clemson, South Carolina 29634

Zhenya Ding
Beijing Graduate School of Wuhan University of Technology, Beijing 100024, China

(Received 3 March 1999; accepted for publication 16 March 1999)

Polar, nonferroelectric $(Ba_xSr_{2-x})TiSi_2O_8$ glass ceramics with highly oriented crystallites were prepared by a gradient temperature heat treatment technique. The crystallization mechanism and microstructures of $(Ba_xSr_{2-x})TiSi_2O_8$ glass ceramics were investigated by means of differential thermal analysis, x-ray diffraction and scanning electron microscopy, and the dielectric, piezoelectric and pyroelectric properties were investigated for various compositions. The results show that polar $(Ba_xSr_{2-x})TiSi_2O_8$ glass ceramics have a low dielectric constant and a high hydrostatic figure of merit $d_h \times g_h = \sim 2500$. This high hydrostatic figure of merit, along with other unique characteristics, such as no aging or depoling problems and good stability at high temperatures, high pressure, and in harsh environments, makes $(Ba_xSr_{2-x})TiSi_2O_8$ glass ceramics attractive for use as hydrophones and high temperature infrared detectors. © *1999 American Institute of Physics.* [S0021-8979(99)06712-2]

I. INTRODUCTION

Piezoelectric ceramics attract a lot of attention because these materials have been used for various electronic devices, particularly electromechanical actuators and sensors. Different perovskite systems, such as barium titanate ($BaTiO_3$) and lead zirconate titanate (PZT) have been successfully developed to meet the needs of numerous applications.[1] Usually, these piezoelectric ceramics are prepared by the sintering of the ceramic powders, which leads to a polycrystalline microstructure. The resulting ceramics are macroscopically isotropic after cooling below the Curie temperature, and exhibit no directional behavior such as macroscopic piezoelectricity or pyroelectricity, unless the ceramics are polarized to make them active under an electric field. However, piezoelectric materials inevitably face aging problems associated with domain wall movement after the poling process.[1] The aging of the materials leads to a degradation of the piezoelectric and pyroelectric properties, and the failure of the devices.

In order to avoid this problem, a novel idea[2] was proposed to prepare piezoelectric and pyroelectric materials which do not require poling. Halliyal[3] explored the possibility of preparing grain-oriented materials with piezoelectric and pyroelectric properties and obtained some positive results. This article reports research on polar, grain-oriented glass ceramics in the system xBaO–$(2-x)$SrO–TiO_2–$3SiO_2$. Results are presented on the crystallization mechanism, grain oriented growth, and piezoelectric and pyroelectric properties of these materials.

II. EXPERIMENT

A. Glass formation and grain-oriented growth

In order to possess piezoelectric and pyroelectric properties, the main crystalline phase in the glass ceramic must be polar in nature. Because of the requirements of the main crystal phase and need for glass formation, the glass system xBaO–$(2-x)$SrO–TiO_2–$3SiO_2$ (BSTS) was selected. SiO_2 (Shanghai Chemical Co.) was used as the glass former and TiO_2 (Beijing Chemical Co., P. R. China) acted as the nucleating agent. $BaCO_3$ and $SrCO_3$ (Beijing Chemical Co., P. R. China) were used to promote the growth of $Ba_xSr_{2-x}TiSi_2O_8$ polar crystallites during the glass crystallization. The glasses in the present study were obtained by mixing and melting the above starting materials with different ratios in a platinum crucible at 1480 °C for 10 h. Transparent cylindrical glass samples with a diameter of 3 cm and a height of 2 cm were obtained by pouring the melt into a preheated graphite mold. After the top and bottom surfaces of the cylindrical samples were carefully polished, the samples were put on a gradient temperature hot stage for grain-oriented crystallization. In the gradient temperature hot stage, the polished bottom ends of samples were placed on an Al_2O_3 substrate at which a maximum temperature of 1020 °C was maintained, and a temperature gradient of 300 °C was achieved along the samples through a 3 cm distance. At the beginning, the samples started to crystallize on the bottom surface and then crystallization proceeded inside the samples slowly. After the 15 h crystallization, highly oriented glass ceramics were obtained.[4] Subsequently, the samples were cut into 2 mm thick disks for property measurements.

B. Sample characterization

The crystallization behavior was determined by a CR-G DTA analyzer at different heating rates with α-Al_2O_3 powder as a reference. The crystalline phases in the glass ceramics were identified by a D/max-IV polycrystalline diffractometer. An ASM-SX scanning electron microscope was used to examine the microstructure and grain orientation of the BSTS glass ceramics.

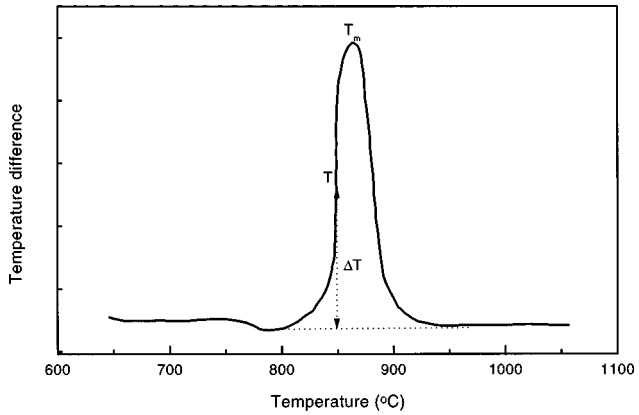

FIG. 1. DTA curve of $(Ba_{1.8}Sr_{0.2})TiSi_2O_8$ glass ceramic at a heating rate of 20 °C/min.

For dielectric, piezoelectric, and pyroelectric property measurements, samples were cut from cylindrical glass ceramics normal to the direction of the temperature gradient. Gold electrodes were deposited on the samples via sputtering. The piezoelectric coefficient d_{33} was measured with a quasistatic piezoelectric d_{33} meter (Model ZJ-2).[5] The dielectric constant and dielectric loss were measured using an HP 4192A impedance analyzer, and the piezoelectric d_{31} constant, electromechanical planar coupling factor k_p, and thickness coupling factor k_t, were calculated from the admittance–frequency curves. The pyroelectric coefficient p_3 was measured by a modified glass method.[6]

III. RESULTS AND DISCUSSION

A. Crystallization mechanism and grain orientation growth

Among the 32 point groups, only the 20 noncentrosymmetric, polar crystal systems[7] may demonstrate piezoelectric behavior. Of these 20 groups, only ten groups are pyroelectric, i.e., they demonstrate a spontaneous polarization. Based on this criterion, in order to possess piezoelectric and pyroelectric properties, the main crystallites of the glass ceramics must be spontaneously polarized. In this work, the polar, noncentrosymmetric fresnoite crystal phase[8] $(Ba_xSr_{2-x})TiSi_2O_8$, tetragonal space group $P4bm$, was chosen as the main crystalline phase by using the proper starting materials.

In addition to the requirement of a polar crystalline phase, the nucleation and growth behavior of the glass ceramics, as well as the spatial distribution of the polar crystallites will have a significant effect on the piezoelectric and pyroelectric properties of BSTS glass ceramics. In order to examine the crystallization mechanism, differential thermal analysis (DTA) curves for the composition $(Ba_{1.8}Sr_{0.2})TiSi_2O_8$ ($x=1.8$) at heating rates of 1, 2, 5, 10, and 20 °C/min were obtained. It is well known that the nucleation and growth behavior of glasses can be described by the Johnson–Mehl–Avrami equation:[9–13]

$$y(t)=1-\exp(-K\times t^n), \tag{1}$$

TABLE I. Crystallization peak temperature T_m at different heating rates for the glass-ceramic system 1.8 BaO–0.2 SrO–TiO_2–3 SiO_2.

Heating rate (°C/min)	1	2	5	10	20
T_m (°C)	812	827	842	862	878

where $y(t)$ is the fraction transformed from the amorphous phase to the crystalline phase at time t, n represents the crystallization index, and K is a function of temperature and can be defined as: $K=A\exp(-E/RT)$. Based on the above equation and DTA curves obtained at different heating rates, two more useful equations[10,11,14] can be derived as

$$\log \Delta T=-\frac{nE}{4.57}\times\frac{1}{T}+C_1, \tag{2}$$

and

$$\log H=-\frac{E}{4.57}\times\frac{1}{T_m}+C_2, \tag{3}$$

where E is the crystallization activation energy, ΔT is the temperature difference at a given temperature T in the DTA curve shown in Fig. 1, T_m is the crystallization peak temperature of the DTA curve at different heating rates H, and C_1 and C_2 are constants.

The crystallization peak temperatures T_m at different heating rates H, are listed in Table I. Several sets of T and ΔT values were obtained by selecting several points around the exothermic peak of the DTA curve in Fig. 1. Subsequently, after plotting $\log \Delta T$ vs $1/T$, and $\log H$ vs $1/T_m$ (Figs. 2 and 3), the crystallization activation energy E, and the crystallization index n were calculated from the slopes of the two plots as:

$$E=238.3 \text{ kJ/mol}, \quad n=2.9$$

According to Table II,[14] which lists the relationships between the crystallization mechanisms and crystallization indices, and the calculated crystallization index of BSTS glass ceramics, we can conclude that the BSTS glass ceramics experienced a crystallization process controlled by interface

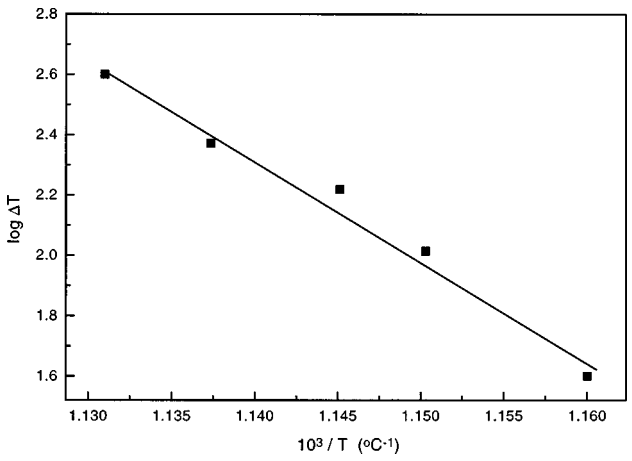

FIG. 2. Plot of $\log \Delta T$ vs $1/T$.

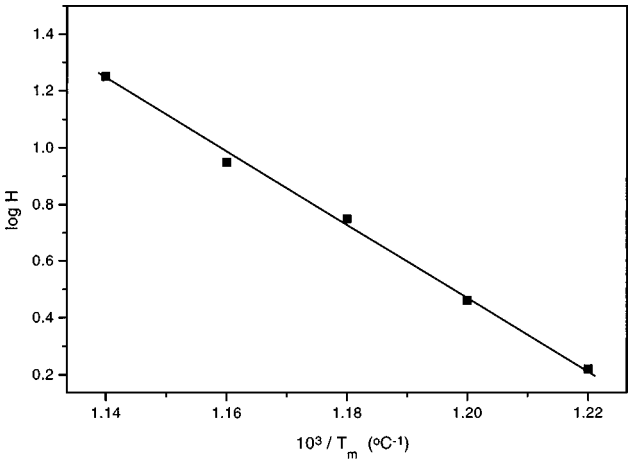

FIG. 3. Plot of $\log H$ vs $1/T_m$.

(surface) with a fixed number of nuclei. This result agrees with our experimental observations. It was found that the samples started to crystallize at the surface and the crystallization proceeded inside the samples along the direction of temperature gradient. On the other hand, because of a certain amount of nucleating agent in the BSTS glass ceramics such as TiO_2, a major nucleating agent, it is reasonable to consider the number of nuclei as a fixed number. This conclusion is useful to control the crystal size by controlling the density of nucleation sites via the inclusion of nucleating agents such as TiO_2, in the glass systems.

Figure 4 shows the x-ray powder diffraction patterns for different compositions after a 15 h full crystallization at a temperature of 1020 °C. It is noted that all of the samples with different compositions, $x=0.2$, 1.2, 1.4, 1.6, 1.8, and 2.0, showed a single phase structure. The main crystal phase was identified as the fresnoite-type $(Ba_xSr_{2-x})TiSi_2O_8$ polar crystal phase. It is believed that the BSTS system exhibits solid solution behavior and all phases such as $Ba_2TiSi_2O_8$, $Sr_2TiSi_2O_8$, and $(Ba_xSr_{2-x})TiSi_2O_8$ have the same crystal symmetry. Therefore, these samples all show the same basic XRD pattern.

The surface XRD patterns taken normal to the gradient temperature for samples with different compositions after 15 h gradient heat treatments are shown in Fig. 5. It is found that the (002) peak is the strongest for all samples, which indicates that the $(Ba_xSr_{2-x})TiSi_2O_8$ crystallites grow with the *C* axis parallel to the temperature gradient.

TABLE II. Crystallization mechanisms and crystallization index *n* (after Marotta *et al.*).[a]

Crystallization mechanisms		Crystallization index *n*
Crystal growth controlled by interface	Constant nucleation rate	4
	Fixed number of nuclei	3
Crystal growth controlled by diffusion	Constant nucleation rate	5/2
	Fixed number of nuclei	3/2

[a]See Ref. 14.

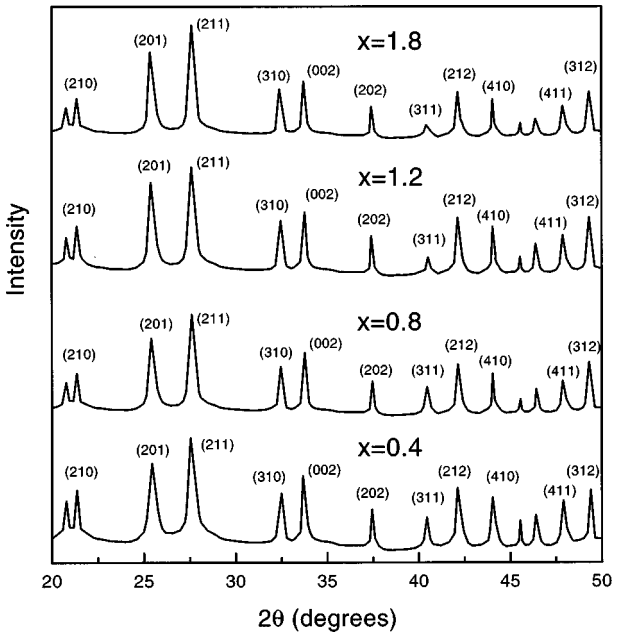

FIG. 4. XRD powder patterns of BSTS glass ceramics with different BaO molar fractions.

Figure 6 shows scanning electron microscopy (SEM) cross-sectional microstructures of BSTS glass ceramics at different heat treatment conditions for the composition $(Ba_{1.8}Sr_{0.2})TiSi_2O_8$. Figure 6(a) shows a sample with 5 h heat treatment in the gradient temperature. It is clear that this sample is not fully crystallized and the piezoelectric d_{33} constant is low $(0.8\times10^{-12}\,C/N)$. After a longer time (8 h) heat treatment, the sample shown in Fig. 6(b) demonstrates more extensive nucleation and growth and relatively higher piezoelectric d_{33} constant $(5.5\times10^{-12}\,C/N)$ in comparison to the first sample, but the crystallization is still incomplete. Figure

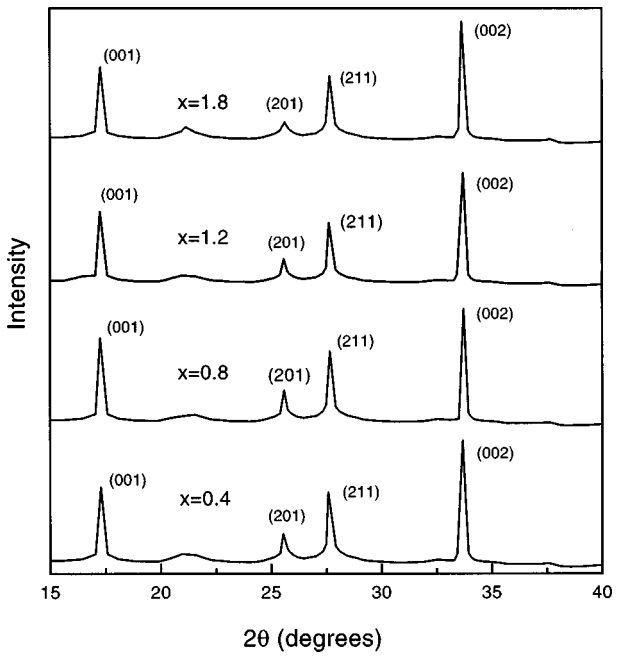

FIG. 5. XRD patterns of glass-ceramic surfaces normal to the temperature gradient for BSTS samples with different BaO molar fractions.

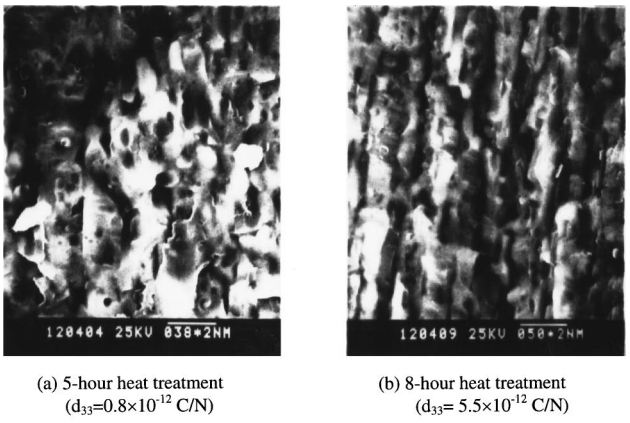

(a) 5-hour heat treatment (d_{33}=0.8×10^{-12} C/N)

(b) 8-hour heat treatment (d_{33}= 5.5×10^{-12} C/N)

(c) 12-hour heat treatment (d_{33}=10.8×10^{-12} C/N)

(d) 15-hour heat treatment (d_{33}=16×10^{-12} C/N)

FIG. 6. Cross-sectional SEM micrographs of BSTS glass ceramics in the system 1.8BaO–0.2SrO–TiO_2–3SiO_2: (a) 5 h, (b) 8 h, (c) 12 h, and (d) 15 h heat treatments. The temperature gradient direction is along the vertical direction in the micrographs.

6(c) (12 h heat treatment) shows small crystallites with good orientation and higher piezoelectric d_{33} constant (10.8×10^{-12} C/N), but a large amount of amorphous material still exists around the crystallites. This indicates that the crystallization process is still not complete after 12 h of heat treatment. The sample in Fig. 6(d) shows excellent grain orientation with a grain size of 5–7 μm after a 15 h gradient temperature heat treatment. The columnal crystallites in the sample formed a dense microstructure with only a small amount of amorphous phase among the crystallites. This sample showed the highest piezoelectric d_{33} constant (16×10^{-12} C/N) among the four samples. These results indicate that the piezoelectric d_{33} constant is strongly dependent on the volume fraction of the oriented fresnoite phase and the orientation of $(Ba_xSr_{2-x})TiSi_2O_8$ crystallites in the glass ceramics.

B. Dielectric and piezoelectric properties

Grain-oriented BSTS glass ceramics with different compositions in the system xBaO–$(2-x)$SrO–TiO_2–3SiO_2 were prepared, and the dielectric and piezoelectric properties were measured as a function of composition. Figure 7 shows the dielectric constant and dielectric loss of BSTS glass ceramics at room temperature for different compositions. It is noted that the dielectric constant for different compositions from $x=0.2$ to $x=2.0$ is about 10–12 with no significant

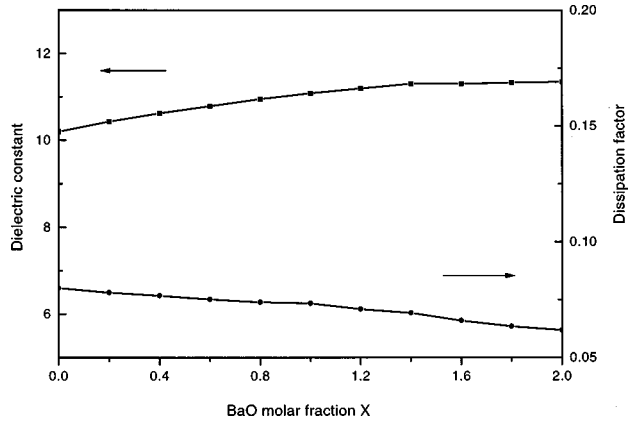

FIG. 7. Compositional dependence of the dielectric constant and dielectric loss of BSTS glass ceramics after 15 h heat treatment.

effect of composition observed. However, the dissipation factor decreases slightly from 0.08 to 0.05 when the value of x is increased from 0.0 to 2.0. It is believed that the similar dielectric properties for the different compositions are attributable to the similar crystal structures of these materials as shown by the XRD patterns in Fig. 4. The compositional dependencies of the piezoelectric d_{33} constant and the planar coupling coefficient k_p are shown in Fig. 8. The maximum d_{33} value was found to be 16×10^{-12} C/N when the BaO molar fraction $x=1.8$. However, the k_p decreased from 10% to 7.6% when the x value increased from 0.0 to 2.0. The change of the d_{33} and k_p values may be caused by the substitution of Ba^{2+} by Sr^{2+} in the solid solution. When Ba^{2+} (larger radius) is replaced by Sr^{2+} (smaller radius), the crystal structure will contract from $Ba_2TiSi_2O_8$ to $Ba_xSr_{(2-x)}TiSi_2O_8$. This slight distortion of the crystal structure may lead to the change of the piezoelectric properties, which are known to strongly depend on the crystal structure.

Figures 9 and 10 show representative admittance–frequency curves for the composition 1.8BaO–0.2SrO–TiO_2–3SiO_2 from which the piezoelectric constant d_{31}, planar coupling factor k_p, and thickness coupling factor k_t were obtained. The hydrostatic constants d_h and g_h can be calculated by the following equations:[7]

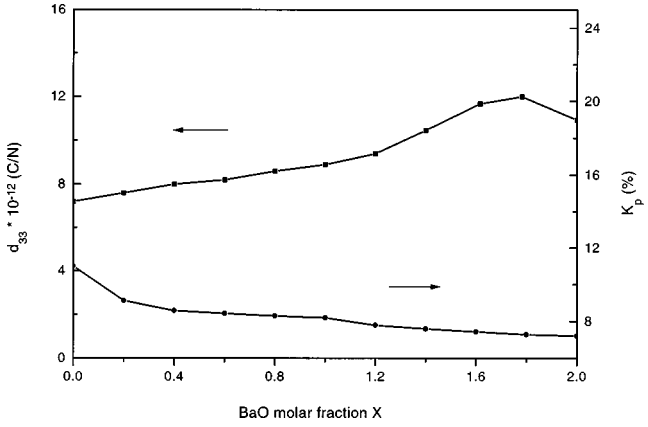

FIG. 8. Compositional dependence of the piezoelectric charge coefficient d_{33} and electromechanical thickness coupling factor k_p after 15 h heat treatment.

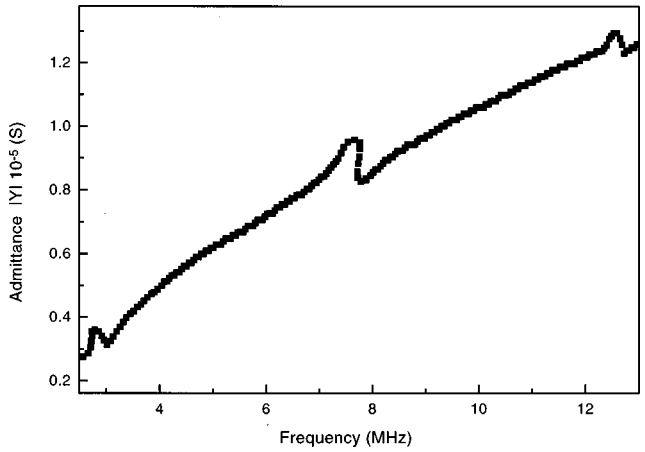

FIG. 9. Plot of admittance vs frequency at the thickness mode for BSTS glass ceramic at a BaO molar ratio of 1.8.

$$d_h = d_{33} + 2d_{31}, \tag{4}$$

$$g_h = d_h / \epsilon_0 K, \tag{5}$$

where K is the dielectric constant and ϵ_0 is the permittivity of free space. The measured and calculated piezoelectric constants d_{33}, d_{31}, d_h, and g_h, and the electromechanical coupling factors k_p and k_t for the composition 1.8BaO–0.2SrO–TiO_2–$3SiO_2$ are listed in Table III. The corresponding properties of lead zirconate titanate (PZT) and polyvinyl fluoride (PVF) are also listed for comparison. As we note, the d_{33} and d_h constants for the BSTS glass ceramics are lower than those of PZT-5 ceramics. However, because of the low dielectric constant of the glass ceramics, the g_{33} and g_h constants of BSTS glass ceramics are much higher than those of PZT-5. In addition, the hydrostatic figure of merit $d_h \times g_h$ for the BSTS glass ceramics is an order of magnitude higher than that of PZT-5.

Because BSTS glass ceramics are nonferroelectric, inorganic materials in nature and there is no poling process involved, no depoling or aging problems[1] are expected. The grain-oriented microstructures of the BSTS glass ceramics were formed at high temperature and the piezoelectric properties associated with the grain-oriented crystallites will be maintained unless the microstructures are destroyed at a high temperature at which the BSTS glass ceramics soften. The nature of inorganic materials also makes BSTS glass ceramics resistant to strong acid, strong base erosion.

TABLE III. Piezoelectric, pyroelectric properties of BSTS glass ceramic, PZT ceramics, and PVF_2 polymer.

Properties	BSTS glass ceramics	PZT-5	PVF_2
K	10–12	1800	13
$d_{33}(10^{-12}$ C/N)	10–16	450	30
$d_{31}(10^{-12}$ C/N)	1–1.4	−205	−18
$d_h(10^{-12}$ C/N)	12–16	40	10
$g_{33}(10^{-3}$ V m/N)	110–130	28	250
$g_h(10^{-3}$ V m/N)	130–160	2.5	100
$d_h \times g_h(10^{-15}$ m^2/N)	1560–2560	100	1000
k_t (%)	30–32	49	19
k_p (%)	4–10.5	34	11.7
P_3 (μC/m^2 K)	4.1–5.8		

Several experiments were done in this study to evaluate the stability of piezoelectric properties with time, under repeatedly heating/cooling cycles, and after exposure to strong acid and base, as well as underwater pressure.[4] It was proved that the BSTS glass ceramics showed no change[4] in the d_{33} constant after a period of 2 years, and exhibited good d_{33} stability when the samples were subjected to ten heating/cooling cycles from 950 to 25 °C. Moreover, the BSTS glass ceramics also demonstrated stable hydrostatic piezoelectric properties, e.g., g_h. The underwater pressure experiment indicated that the g_h constant showed no obvious change when the underwater pressure was increased to 9 MPa. This is because high hydrostatic pressures will not reshape the grain-oriented microstructures which contribute to the piezoelectric properties. It is also found that the BSTS samples demonstrated good resistance to the strong acid and base after being soaked in strong hydrochloric acid (5.0 N HCl) and strong sodium hydroxide solution (4.0 N NaOH) for 2 weeks. No obvious erosion of the samples and change of the piezoelectric constant d_{33} were observed.

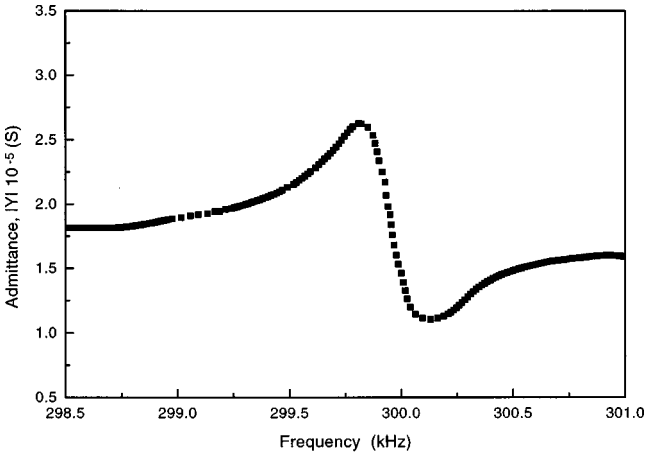

FIG. 10. Plot of admittance vs frequency at the planar mode for BSTS glass ceramic with a BaO molar fraction of 1.8.

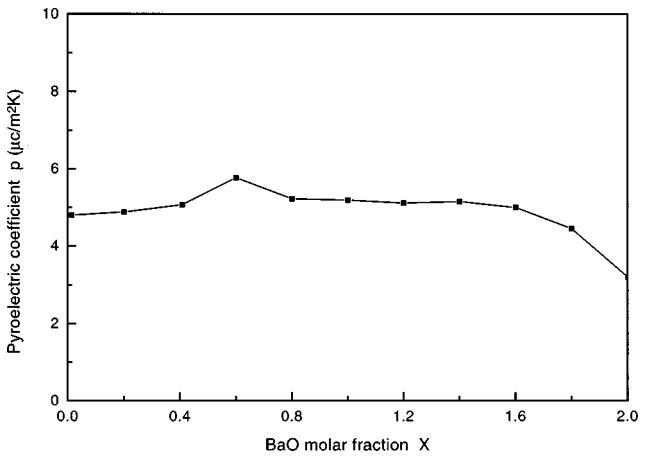

FIG. 11. Composition dependence of the pyroelectric coefficient in BSTS glass ceramics after 15 h heat treatment.

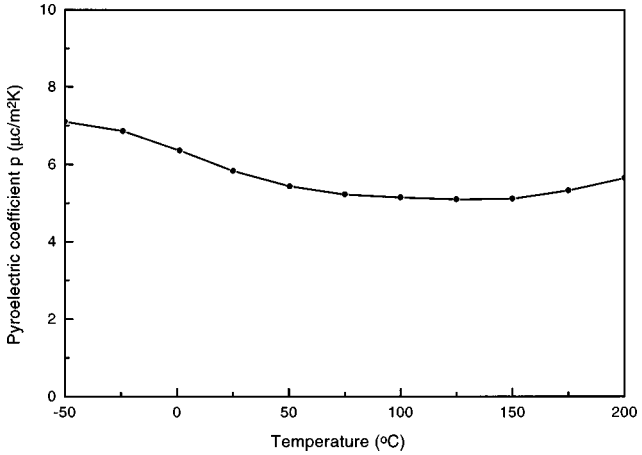

FIG. 12. Temperature dependence of the pyroelectric coefficient for BSTS glass ceramic at a BaO molar ratio of 1.4 after 15 h heat treatment.

In addition to the high hydrostatic figure of merit $d_h \times g_h = \sim 2500$, the strong stability of piezoelectric properties of the BSTS glass ceramics at high temperatures, high pressure, and in harsh environments, makes $(Ba_xSr_{2-x})TiSi_2O_8$ glass ceramics attractive for use as hydrophones.

C. Pyroelectric properties

As for the pyroelectric properties, the composition dependence of the pyroelectric coefficient of BSTS glass ceramics was investigated by measuring the pyroelectric coefficient p_3. It is shown in Fig. 11 that the pyroelectric coefficient reaches a maximum value of 5.8 $\mu C/m^2 K$ at room temperature when $x=0.6$. Figure 12 illustrates the dependence of pyroelectric coefficient on temperature for the system $x=0.6$. It was noted that the BSTS glass ceramics show a positive coefficient in the temperature range from -50 to 200 °C in comparison with the negative pyroelectric coefficient in most single crystals.[8] The reason for this negative pyroelectric coefficient is because the secondary pyroelectric coefficient p_{sec} in this glass-ceramic system is larger than the primary pyroelectric coefficient,[8] p_{prim}. For the point group 4mm, the pyroelectric coefficient can be given by the following relationship:[15]

$$p_i^{\sigma} = (\partial P_s/\partial T)_{E,S} + d_{31}(C_{11}\alpha_1 + C_{12}\alpha_1 + C_{13}\alpha_3) + d_{33}(2C_{13}\alpha_1 + C_{33}\alpha_3), \quad (6)$$

where p_i^{σ} is the total pyroelectric coefficient measured at constant stress and $(\partial P/\partial T)_{E,S}$ is the primary pyroelectric coefficient with a negative sign which is defined by the spontaneous polarization change with temperature. The next two terms are the secondary pyroelectric coefficient with a positive sign which is contributed by the piezoelectric effect because the thermal expansion generates a strain when the temperature changes. d_{31} and d_{33} are the piezoelectric coefficients, C_{11}, C_{12}, and C_{13} represent the elastic stiffness coefficients, and α_1 and α_3 are the linear expansion coefficients in the I and III directions. E, S, and σ represent constant electric field, strain, and stress, respectively. Since the secondary pyroelectric coefficient is larger than the primary pyroelectric coefficient in BSTS glass-ceramics system, the overall pyroelectric coefficient exhibits a positive value.

The pyroelectric coefficients of BSTS glass ceramics at room temperature are smaller than those of commercial pyroelectric materials, such as TGS, $LiNbO_3$, and $LiTaO_3$, but they show several advantages such as high temperature stability and good ability to withstand high power laser radiation.[16] Therefore, they have potential application in high temperature infrared (IR) detectors.

IV. CONCLUSIONS

Nonferroelectric, polar BSTS glass ceramics with piezoelectric and pyroelectric properties were prepared by a gradient temperature technique. Highly oriented $(Ba_xSr_{2-x})TiSi_2O_8$ crystallites were obtained after 15 h of gradient temperature heat treatment and it is believed that the orientation crystallization was controlled by the surfaces of the samples. The piezoelectric properties strongly depend on the crystallite orientation of $(Ba_xSr_{2-x})TiSi_2O_8$. The dielectric, pyroelectric, and piezoelectric measurement results show that the polar BSTS glass ceramics have a low dielectric constant of ~ 12, a low pyroelectric coefficient of 5.8 $\mu C/m^2 K$, and a high hydrostatic figure of merit $d_h \times g_h = \sim 2500$. This high hydrostatic figure of merit, along with other unique characteristics of these materials, such as no aging and no depoling problem, good stability in high temperature, high pressure, and harsh environments, makes BSTS glass ceramics attractive for hydrophone and high temperature IR detector applications.

ACKNOWLEDGMENTS

The authors would like to thank Shuoliu Chen and Youqiu Zhuang of the Institute of Acoustics, Academia Sinica, Beijing, China for help with piezoelectric measurements and Yin Jie of the No. 11 Institute of Electronics Department, Beijing, China for the pyroelectric measurements.

[1] B. Jaffe, W. R. Cook, and H. Jaffe, *Piezoelectric Ceramics* (Academy, New York, 1971).
[2] G. Gardopee, R. Newnham, and A. Halliyal, Appl. Phys. Lett. **36**, 817 (1980a).
[3] A. Halliyal, A. Bhalla, L. Cross, and R. Newnham, J. Mater. Sci. **20**, 3745 (1985).
[4] J. P. Zhang and Z. Ding, J. Chin. Ceram. Soc. **19**, 431 (1991).
[5] P. Chao and S. Chen, Appl. Acoust. **6**, 37 (1987).
[6] A. M. Glass, J. Appl. Phys. **40**, 4699 (1969).
[7] A. Moulson and J. Herbert, *Electroceramics* (Chapman & Hall, London, 1990).
[8] S. Markgraf, A. Halliyal, A. Bhalla, and R. Newnham, Ferroelectrics **62**, 17 (1985).
[9] M. Avrami, J. Chem. Phys. **8**, 212 (1940).
[10] D. Henderson, J. Non-Cryst. Solids **30**, 301 (1979).
[11] H. Borchard and F. Daniels, J. Am. Chem. Soc. **78**, 41 (1957).
[12] J. Briggs and T. Carruthers, Phys. Chem. Glasses **2**, 30 (1976).
[13] W. Hammetter and R. Loehman, J. Am. Ceram. Soc. **70**, 577 (1987).
[14] A. Marotta and A. Buri, Thermochim. Acta **25**, 155 (1978).
[15] A. S. Bhalla and R. E. Newnham, Phys. Status Solidi A **58**, K19 (1980).
[16] J. P. Zhang and Z. Y. Ding, in *Proceedings of 1991 Dalian International Conference on Glass*, edited by Chenyu Wang (Chinese Science and Technology, 1992), p. 123.